СООБЩЕНИЯ
ОБЪЕДИНЕННОГО
ИНСТИТУТА
ЯДЕРНЫХ
ИССЛЕДОВАНИЙ

Дубна

E13-97-215

E.I.Shahaliev, L.M.Soroko

RESOLVING POWER OF THE PHYSICAL DEVICE WITH NONSYMMETRICAL SPREAD FUNCTION

1997

1. Introduction

Usually, the resolving power of the physical device is defined by the width at half maximum of its spread function. For physical device with nonsymmetrical spread function we must take into consideration the second factor — the degree of the nonsymmetricity of the given spread function.

In this paper we consider the resolving power of the physical device with nonsymmetrical spread function. The quality of such physical devices we analyze in term of the Fourier Transformation approach [1,2]. According to this approach the quality of the physical device is defined exhaustively by the Fourier Transform (FT) spectrum of its spread function. This approach has been used for analyze of spectral information in the nuclear physics in [3].

It is shown that physical device with nonsymmetrical spread function has higher resolving power than physical device with symmetrical spread function with the same halfwidth. We have calculated the dependence of the resolving power versus relative noise level ε, from $\varepsilon = 1$, to $\varepsilon = 10^{-3}$, and for different ratio $\kappa = \sigma_L/\sigma_R$, from $\kappa = 1$ to $\kappa = \infty$, where σ_L and σ_R are the left and the right halfwidths of the nonsymmetrical spread functions. The factor of merits of the physical device with nonsymmetrical spread function increases with the experiment quality $1/\varepsilon$ and with ratio $\kappa = \sigma_L/\sigma_R$. The plots of the resolving power are limited by the curve at $\kappa = \infty$. The calculations were made for gaussian and for lorentzian spread functions.

2. Fourier Transformation approach

The Fourier Transformation, $\hat{\mathcal{F}}$, is the transition from the initial function $f(x)$ to its Fourier Transform $F(\omega)$:

$$f(x) \xrightarrow{\hat{\mathcal{F}}} F(\omega) = \int f(x) \exp(-i\omega x) dx\,, \tag{1}$$

ω is the frequency. The inverse Fourier Transformation, $\hat{\mathcal{F}}^{-1}$, from the Fourier Transform $F(\omega)$, to the initial function $f(x)$ is defined as

$$F(\omega) \xrightarrow{\hat{\mathcal{F}}^{-1}} f(\omega) = \int F(\omega) \exp(i\omega x) d\omega\,. \tag{2}$$

The Fourier Transformation (1) can be written as the sum of two partial FT's:

$$F(\omega) = F_{\cos}(\omega) + iF_{\sin}(\omega) \tag{3}$$

where

$$\left.\begin{aligned} F_{\cos} &= \int f(x) \cos(\omega x) dx\,, \\ F_{\sin} &= \int f(x) \sin(-\omega x) dx\,. \end{aligned}\right\} \tag{4}$$

In general case the initial function $f(x)$ can be written as the sum of the even function $F^+(x)$ and the odd function $f^-(x)$:

$$f(x) = f^+(x) + f^-(x), \tag{5}$$

where

$$\left.\begin{aligned} f^+(x) &= \tfrac{1}{2}[f(+x)+f(-x)], \\ f^-(x) &= \tfrac{1}{2}[f(+x)-f(-x)]. \end{aligned}\right\} \tag{6}$$

It is evident that

$$\left.\begin{aligned} F_{\cos}\{f^-(x)\} &\equiv 0, \\ F_{\sin}\{f^+(x)\} &\equiv 0, \end{aligned}\right\} \tag{7}$$

or

$$\left.\begin{aligned} \hat{\mathcal{F}}\{f^+(x)\} &= F_{\cos}(\omega), \\ \hat{\mathcal{F}}\{f^-(x)\} &= f_{\sin}(\omega) \end{aligned}\right\} \tag{8}$$

and

$$\left.\begin{aligned} \hat{\mathcal{F}}^{-1}\{F_{\cos}(\omega)\} &= f^+(x), \\ \hat{\mathcal{F}}^{-1}\{F_{\sin}(\omega)\} &= f^-(x). \end{aligned}\right\} \tag{9}$$

An example of the symmetrical (left) and of the nonsymmetrical (right) spread functions $h(x)$ are shown in Fig. 1 for two different physical devices. As well be explained later, the resolving power of these two physical devices are principally different even for the same halfwidths of their spread functions.

The FT of the gaussian

$$g(x) = \exp(-x^2/2\sigma^2), \tag{10}$$

where σ is the parameter of the gaussian, is equal to

$$F_g(\omega) = \exp(-\omega^2/2\Omega^2), \tag{11}$$

with

$$\Omega\sigma = 1. \tag{12}$$

As an illustration of the reation, eq. (12), we present three different gaussian $g_i(x)$ $(i = 1,2,3)$ and corresponding three FT's in the logarithmical scale (Fig. 2). The sequence of the direct and inverse Fourier Transformations are shown in Fig. 3: Fig. 3a — the initial gaussian, Fig. 3b and Fig. 3c — partial FT's $F_{\cos}$ and $F_{\sin}$. For symmetrical initial function we have $F_{\sin} \equiv 0$. The partial FT $F_{\cos}$ is presented in the logarithmic scale in Fig. 3d. The inverse FT of the $F_{\cos}$ is given in Fig. 3e as even g^+ function. The odd g^- function is equal to zero (Fig. 3f). The initial function $g_s(x)$ is presented in Fig. 3g.

3. Physical device with nonsymmetrical gaussian spread function

The sequence of the direct and inverse Fourier Transformations of the nonsymmetrical gaussian $g_A(x)$ are given in Fig. 4, where

$$g_A(x) = \begin{cases} \exp(-x^2/2\sigma_L^2) & x < 0, \\ \exp(-x^2/2\sigma_R^2) & x > 0. \end{cases} \tag{13}$$

The initial nonsymmetrical gaussian is given in Fig. 4a. The partial FT's, $F_{\cos}$ and $F_{\sin}$, are given in Fig. 4b and Fig. 4c in the linear scale, and in Fig. 4d and Fig. 4e — in the logarithmical scale. The even part of the nonsymmetrical gaussian $g^+(x)$ is presented in Fig. 4f, and the odd part one $g^-(x)$ in Fig. 4g. The sum

$$g_A(x) = g^+(x) + g^-(x) \tag{14}$$

is shown in Fig. 4h.

The computer simulation of the resolving power problem has been performed with the array of six different nonsymmetrical gaussian presented in Fig. 5 for different $\kappa = \sigma_L/\sigma_R$. The complete FT, $|F|$, and the partial FT, $F_{\sin}$, are given in Fig. 6 for first three gaussians (a, b, c) and in Fig. 7 for last three gaussians (d, e, f).

From Figs 6 and 7 we see that the partial FT, $F_{\sin}$, has wings in the region of the middle frequencies ω and that $F_{\sin}$ maximum increases with ratio $\kappa = \sigma_L/\sigma_R$. Both factors increase the intensity of the complete FT, $|F|$, in the region of the middle and high frequencies ω and thus increase the resolving power of the physical device.

The results of the computer simulation are presented in Fig. 8. The FT spectrum width Γ is plotted versus the experiment quality $1/\varepsilon$ for symmetrical gaussian (s), for six nonsymmetrical gaussians (a, b, c, d, e, f) and for completely nonsymmetrical gaussian (lim) with $\kappa = \infty$.

We see that at low values of the experiment quality $1/\varepsilon$ the difference between all these 8 curves is practically absent. This can be explained by very high noise level, when the noise does not allow even to establish the fact, which form, symmetrical or nonsymmetrical, has the spread function of the physical device.

The difference between physical devices is getting pronounced only for the experiment quality $1/\varepsilon \geq 3$. All possible FT spectrum width Γ is restricted from above by the curve "lim", which corresponds to completely nonsymmetrical gaussian with $\kappa = \infty$. The factor of merits of the physical device with nonsymmetrical gaussian

spread function over the physical device with symmetrical spread function is equal to 3.16:1 for $\varepsilon = 1/20$ and $\kappa = 12.06$, and is equal to 2.05:1 for $\varepsilon = 10^{-2}$ and $\kappa = 3.508$.

4. Physical device with nonsymmetrical lorentzian spread function

Now we consider resolving power of the physical device with nonsymmetrical lorentzian spread function. In Fig. 9 we show at first the sequence of the direct and inverse Fourier Transformations of the symmetrical lorentzian $f_s(x)$:

$$f_s(x) = \frac{1}{x^2 + \sigma^2}, \tag{15}$$

where σ is the parameter (Fig. 9a). The partial FT's, $F_{\cos}$ and $F_{\sin}$, are shown in Fig. 9b and Fig. 9c. The partial FT, $F_{\cos}$, in the logarithmic scale presented in Fig. 9d, has remarkable linear dependence versus frequency ω. The even part f^+ and the odd part $f^- \equiv 0$ of the initial symmetrical lorentzian are shown in Fig. 9e and Fig. 9f. The sum

$$f_s(x) = f^+(x) + f^-(x) \tag{16}$$

is given in Fig. 9g.

In Fig. 10 we show the sequence of the direct and inverse Fourier Transformations of the nonsymmetrical lorentzian $f_A(x)$:

$$f_A(x) = \begin{cases} \frac{1}{x^2+\sigma_L^2}, & x < 0, \\ \left(\frac{\sigma_R^2}{\sigma_L^2}\right)\frac{1}{x^2+\sigma_R^2}, & x > 0. \end{cases} \tag{17}$$

The initial nonsymmetrical lorentzian for $\kappa = \sigma_L/\sigma_R = 3.5$ is shown in Fig. 10a. The partial FT's, $F_{\cos}$ and $F_{\sin}$, of $f_A(x)$ are presented in Fig. 10b and Fig. 10c. Now the dependence $\ln|F_{\cos}|$, presented in Fig. 10d, has complex structure. There is a narrow part with quasilinear dependence at low frequency ω with slope which is defined by the σ_L. At very high frequency ω we observe the quasilinear dependence with slope, defined by the σ_R. The plot $|F_{\sin}|$ has deep minima (Fig. 10e). The even part f_A^+ and the odd part f_A^- of the initial nonsymmetrical lorentzian are shown in Fig. 10f and Fig. 10g. The sum

$$f_A(x) = f_A^+(x) + f_A^-(x), \tag{18}$$

is given in Fig. 10h.

The computer simulation of the resolving power problem has been performed with array of six different nonsymmetrical lorentzians presented in Fig. 11 for different $\kappa = \sigma_L/\sigma_R$. The complete FT, $|F|$, and the partial FT, $F_{\sin}$ are given in Fig. 12 for first three lorentzians (a, b, c), and in Fig. 13 for last three lorentzians (d, e, f).

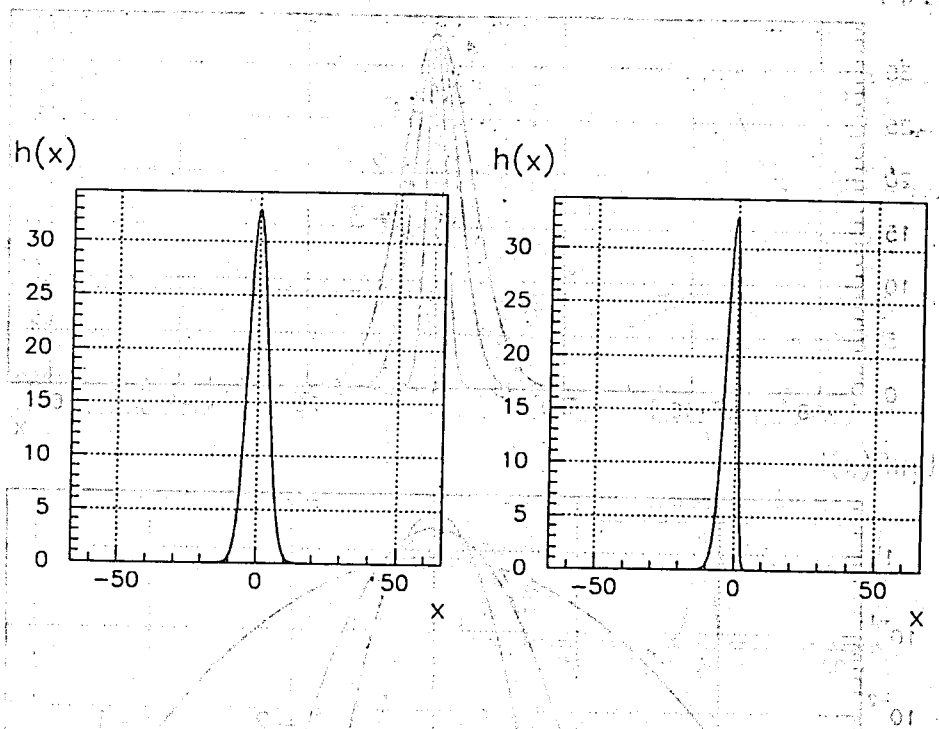

Fig. 1. Symmetrical $h_s(x)$ and nonsymmetrical $h_A(x)$ spread functions of the phy ical devices.

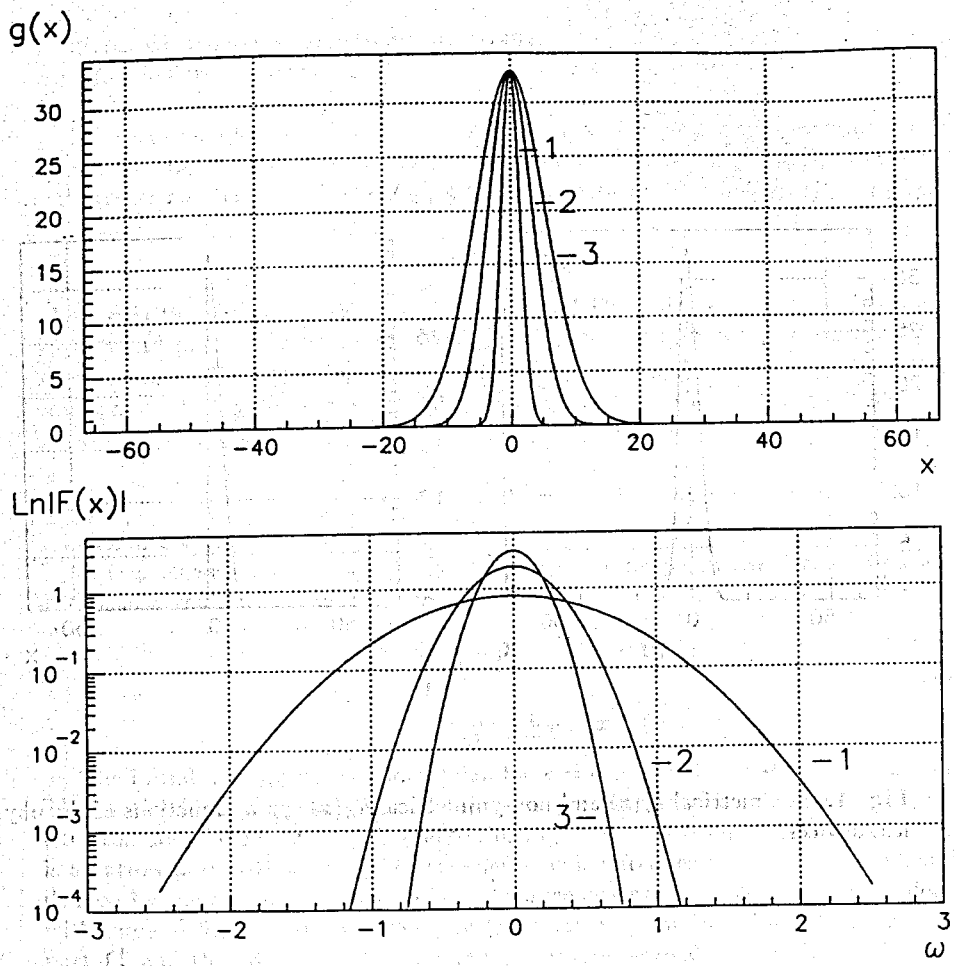

Fig. 2. Symmetrical gaussian spread functions $g(x)$ $(i = 1, 2, 3)$, and their Fourier Transforms in the logarithmic scale $\ln |F(\omega)|$ $i = 1, 2, 3$.

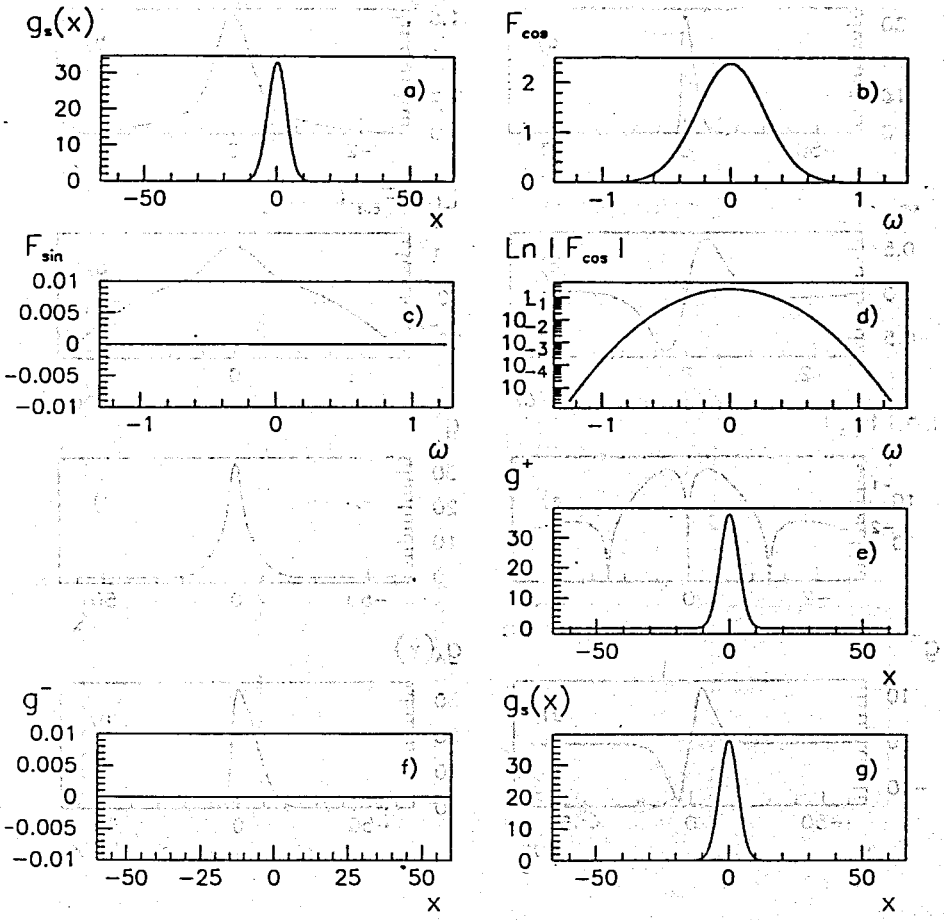

Fig. 3. Sequence of the direct and of the inverse Fourier Transformations of the symmetrical gaussian spread function $g_s(x)$: a) the given symmetrical spread function $g_s(x)$; b) the partial FT, $F_{\cos}$, of the symmetrical gaussian $g_s(x)$; c) the partial FT, $F_{\sin}$; d) $\ln |F_{\cos}|$; e) inverse FT of the partial FT, $F_{\cos}|$, $g^+(x)$; f) inverse FT of the partial FT, $F_{\sin}$, $g^-(x)$; g) the sum of the $g^+(x)$ and $g^-(x)$ which is equal to the initial symmetrical gaussian $g_s(x)$.

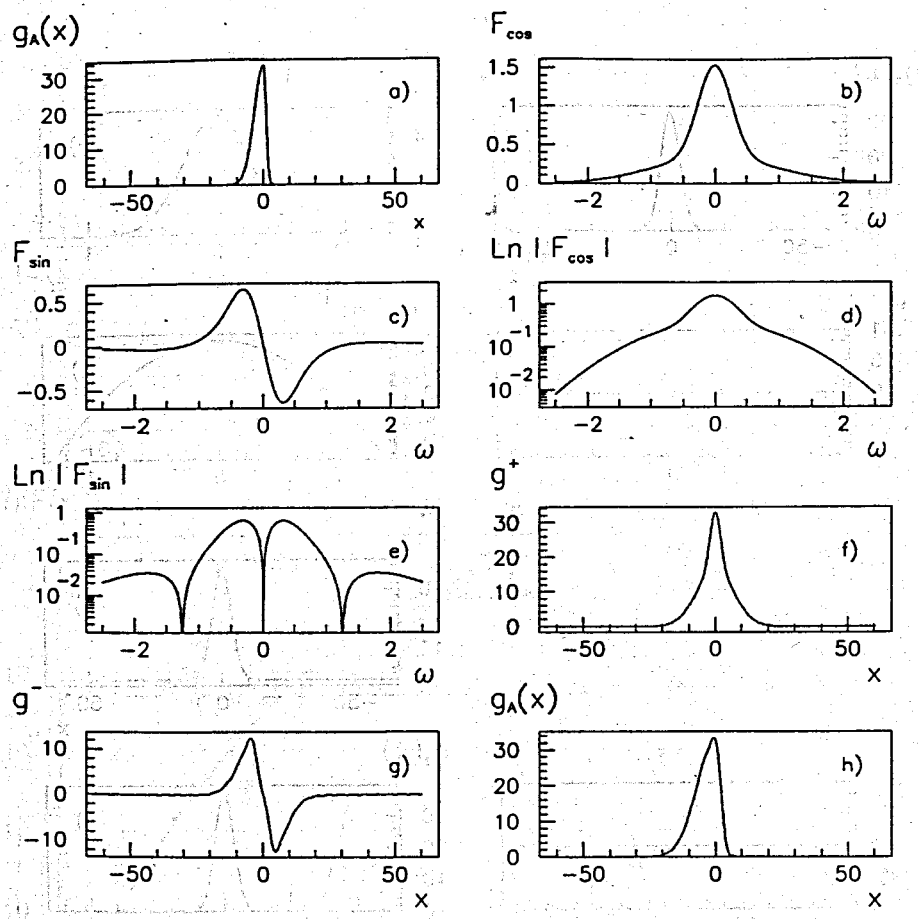

Fig. 4. Sequence of the direct and of the inverse Fourier Transformations of the nonsymmetrical gaussian spread function $g_A(x)$: a) the given nonsymmetrical spread function $g_A(x)$; b) the partial FT, $F_{\cos}$, of the nonsymmetrical gaussian $g_a(x)$; c) the partial FT, $F_{\sin}$, of the $g_A(x)$; d) $\ln|F_{\cos}|$; e) $\ln|F_{\sin}|$; f) inverse FT of the $F_{\cos}$, $g_A^+(x)$; g) inverse FT of the $F_{\sin}$, $g_a^-(x)$; h) the sum of the $g_A^+(x)$ and $g_A^-(x)$ which is equal to the initial nonsymmetrical gaussian $g_A(x)$.

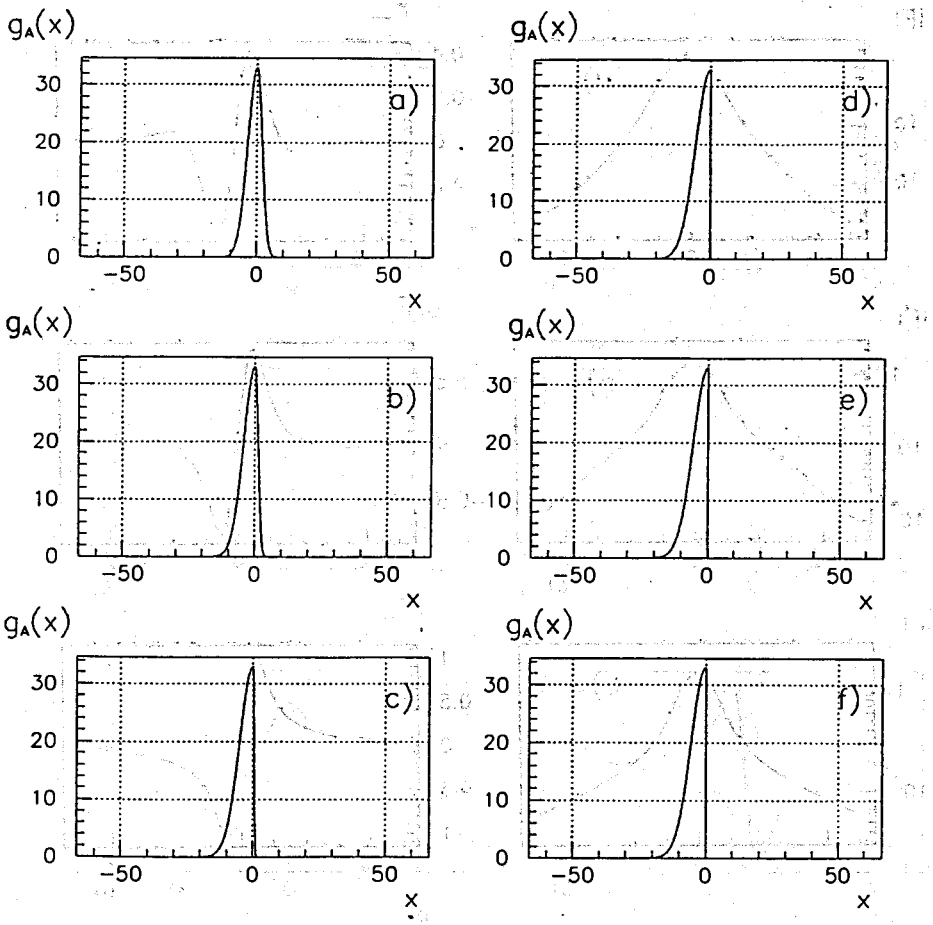

Fig. 5. The array of six different nonsymmetrical gaussian spread functions, used in the computer simulation, with following parameters:

	a	b	c	d	e	f
σ_L	3.5	4.28	5.08	5.35	5.45	5.48
σ_R	2.0	1.22	0.42	0.15	0.05	0.02

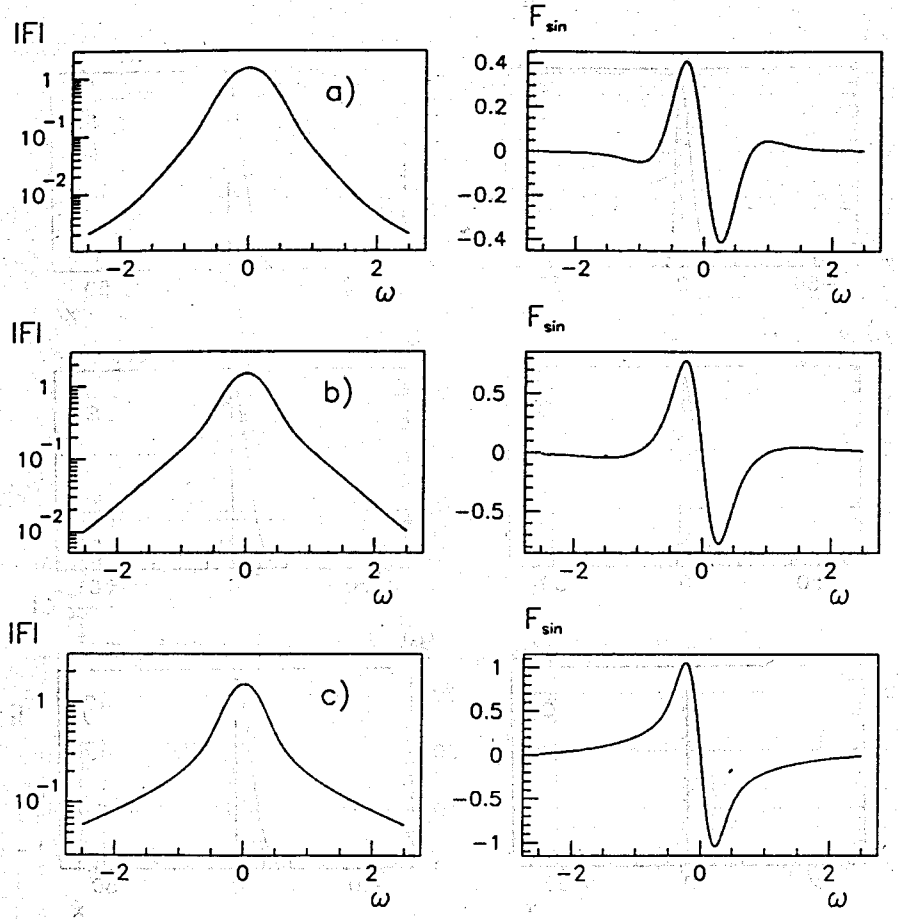

Fig. 6. The complete FT, $|F|$, and the partial FT, $F_{\sin}$, of the nonysmmetrical gaussian spread functions, shown in Fig. 5, for first three parameters:

	a	b	c
σ_L	3.5	4.28	5.08
σ_R	2.0	1.22	0.42

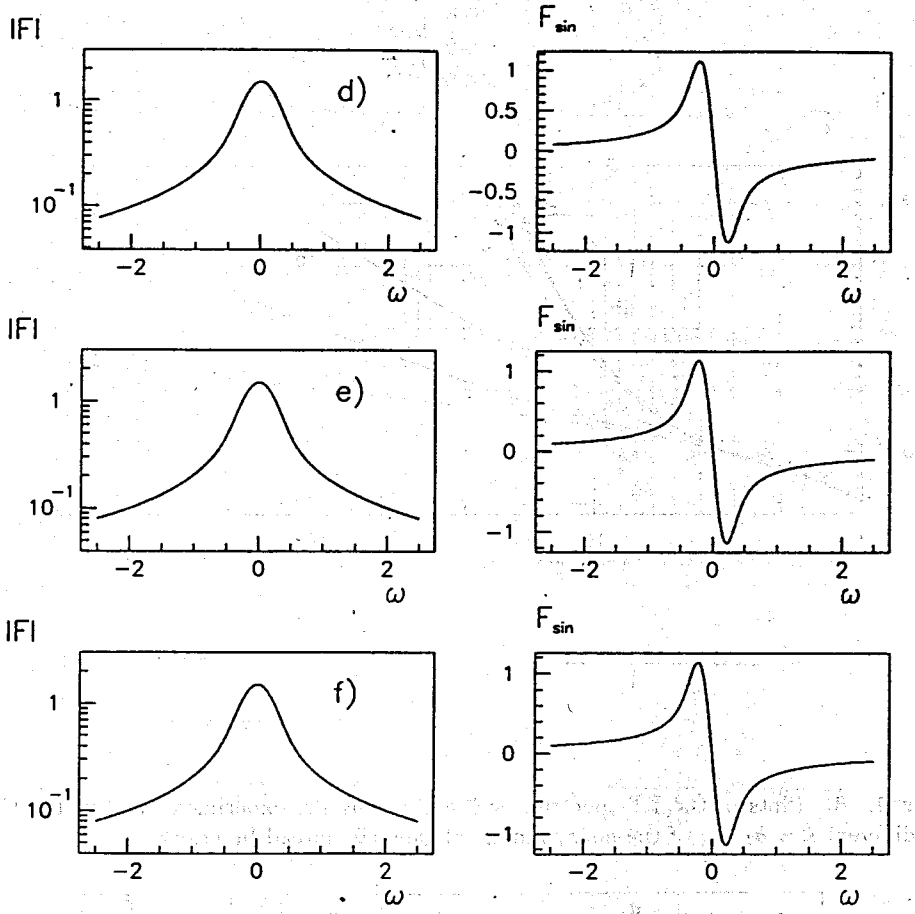

Fig. 7. The complete FT, $|F|$, and the partial FT, $F_{\sin}$, of the nonsymmetrica gaussian spread functions, shown in Fig. 5, for last three parameters:

	d	e	f
σ_L	5.35	5.45	5.48
σ_R	0.15	0.05	0.02

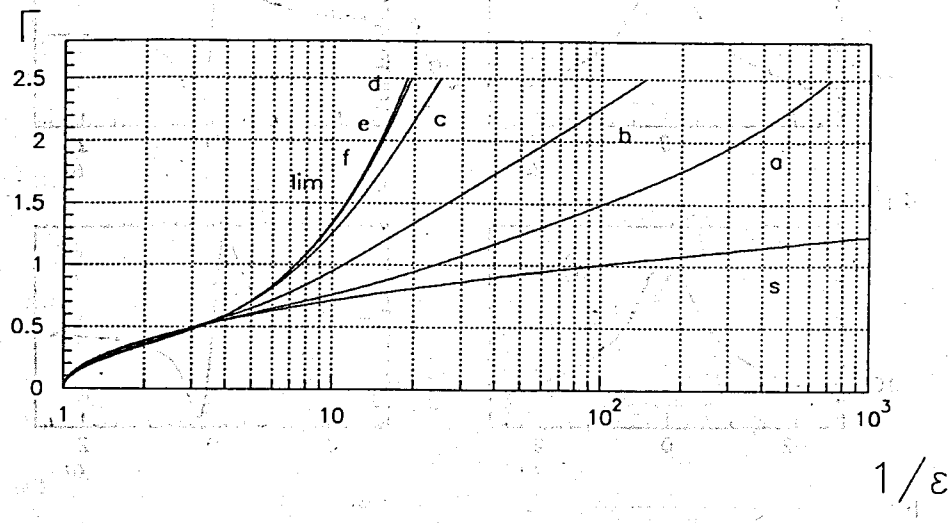

Fig. 8. Plots of the FT spectrum width Γ versus the experiment quality $1/\varepsilon$ for different $\kappa = \sigma_L/\sigma_R$ of the nonsymmetrical gaussian spread function:

	a	b	c	d	e	f
$\kappa = \sigma_L/\sigma_R$	1.75	3.508	12.096	35.67	109.0	274.0

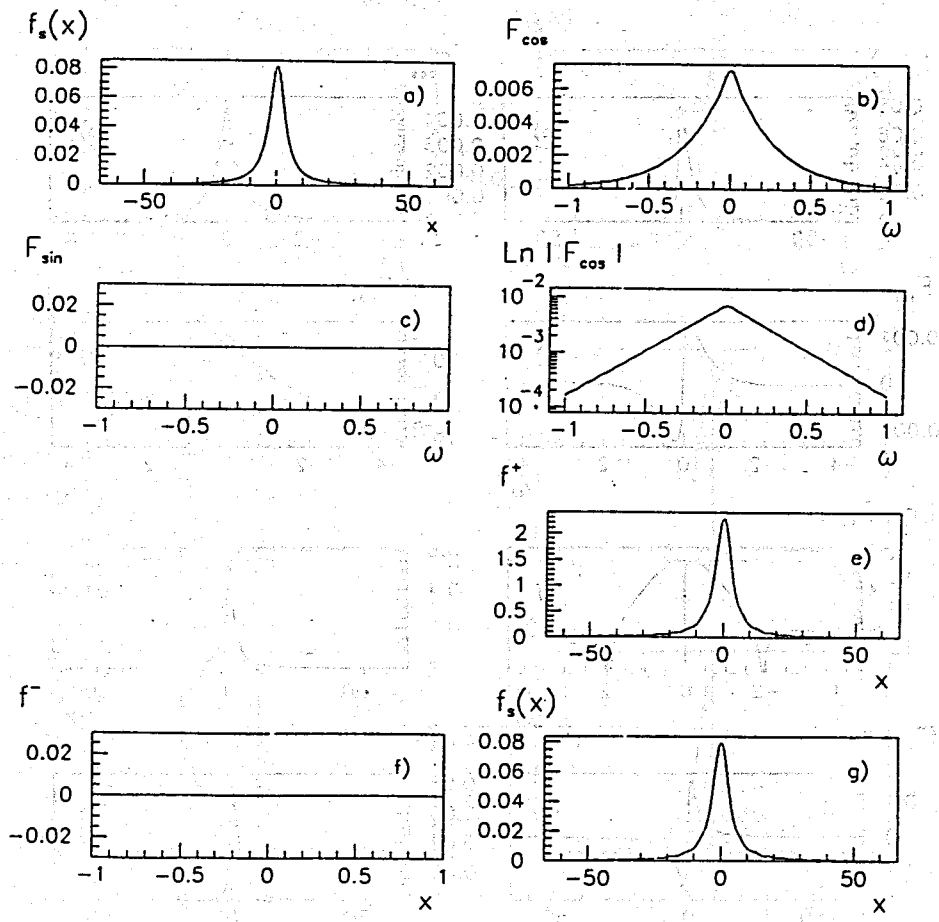

Fig. 9. Sequency of the direct and of the inverse Fourier Transformations of the symmetrical lorentzian spread function $f_s(x)$: a) the given symmetrical spread function $f_s(x)$; b) the partial FT, $F_{\cos}$, of the symmetrical lorentzian $f_s(x)$; c) the partial FT, $F_{\sin}$; d) $\ln|F_{\cos}|$; e) inverse FT of the partial FT, $F_{\cos}$, $f_s^+(x)$; f) inverse FT of the partial FT, $F_{\sin}$, $f_s^-(x)$; g) the sum of the $f_s^+(x)$ and $f_s^-(x)$ which is equal to the initial symmetrical lorentzian $f_s(x)$.

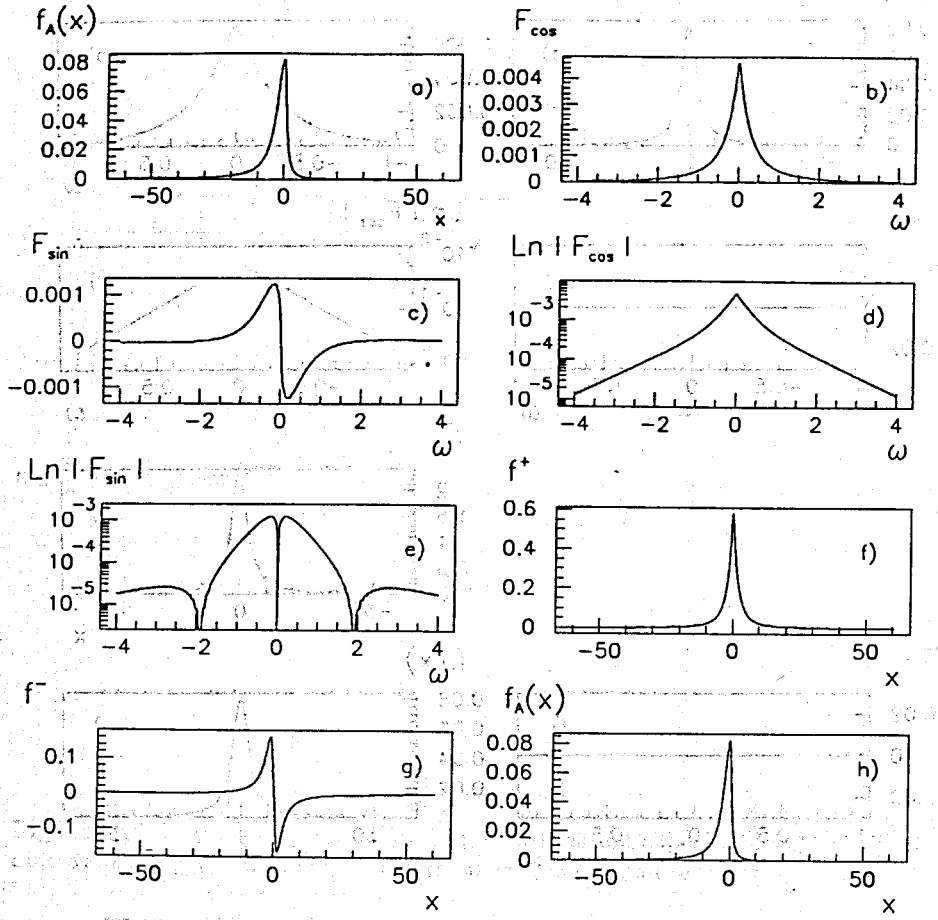

Fig. 10. Sequence of the direct and of the inverse Fourier Transformations of the nonsymmetrical lorentzian spread function $f_A(x)$: a) the given nonsymmetrical spread function $f_A(x)$; b) the partial FT, $F_{\cos}$, of the nonsymmetrical lorentzian $f_A(x)$; c) the partial FT, $F_{\sin}$, of the $f_A(x)$; d) $\ln|F_{\cos}|$; e) $\ln|F_{\sin}|$; f) the inverse FT of the $F_{\cos}$, $f_A^+(x)$; g) the inverse FT of the $F_{\sin}$, $f_A^-(x)$; h) the sum of the $f_A^+(x)$ and $f_A^-(x)$ which is equal to the initial nonsymemtrical lorentzian $f_A(x)$.

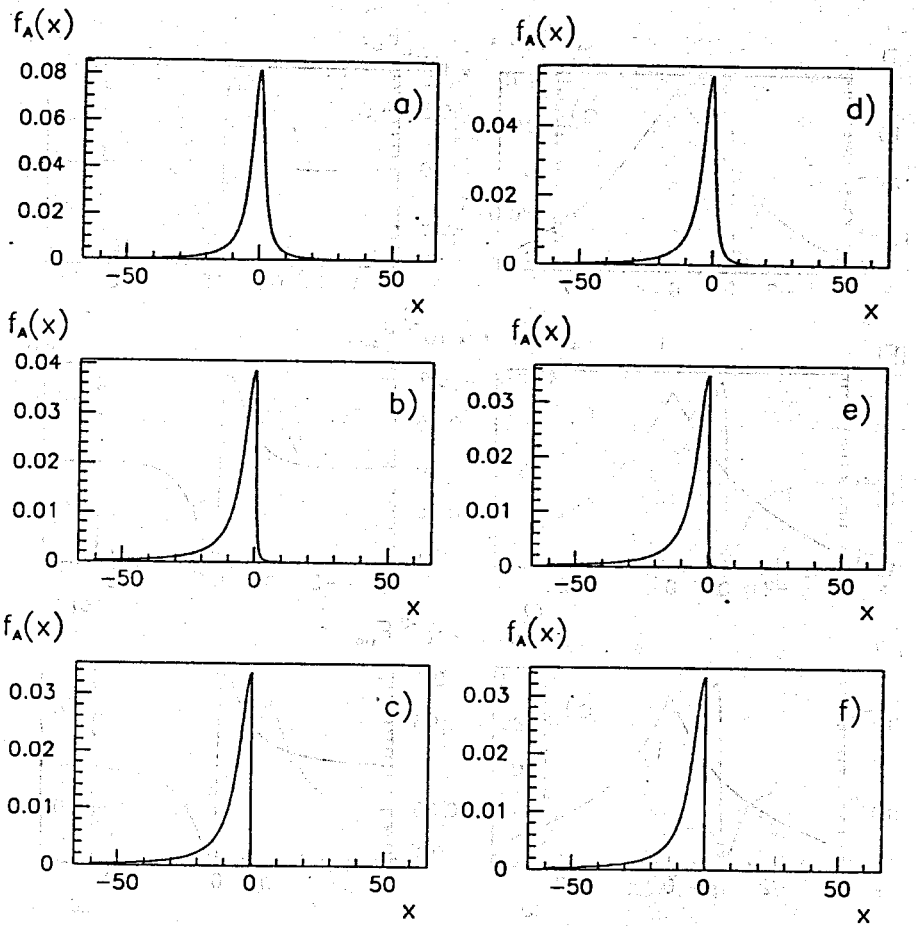

Fig. 11. The array of the different nonsymmetrical lorentzian spread functions, used in the computer simulation, with following parameters:

	a	b	c	d	e	f
σ_L	3.5	4.28	5.08	5.35	5.45	5.48
σ_R	2.0	1.22	0.42	0.15	0.05	0.02

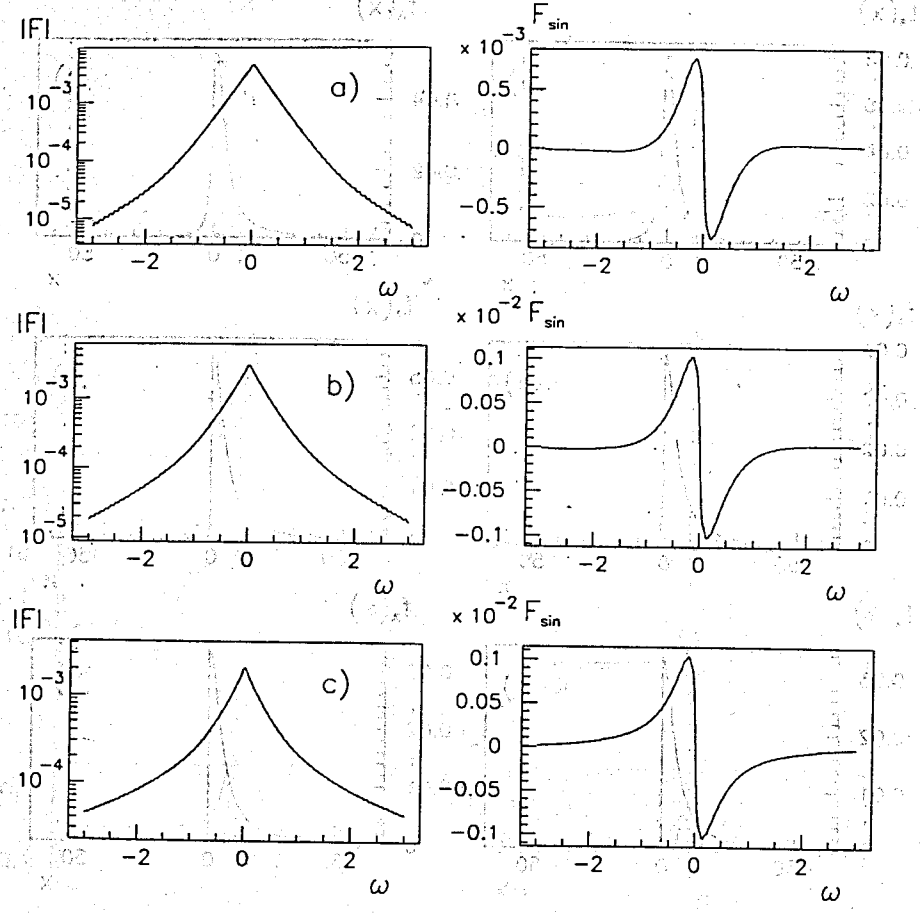

Fig. 12. The complete FT, $|F|$, and the partial FT, $F_{\sin}$, of the nonsymmetrical lorentzian spread functions, shown in Fig. 11, for first three parameter:

	a	b	c
σ_L	3.5	4.28	5.08
σ_R	2.0	1.22	0.42

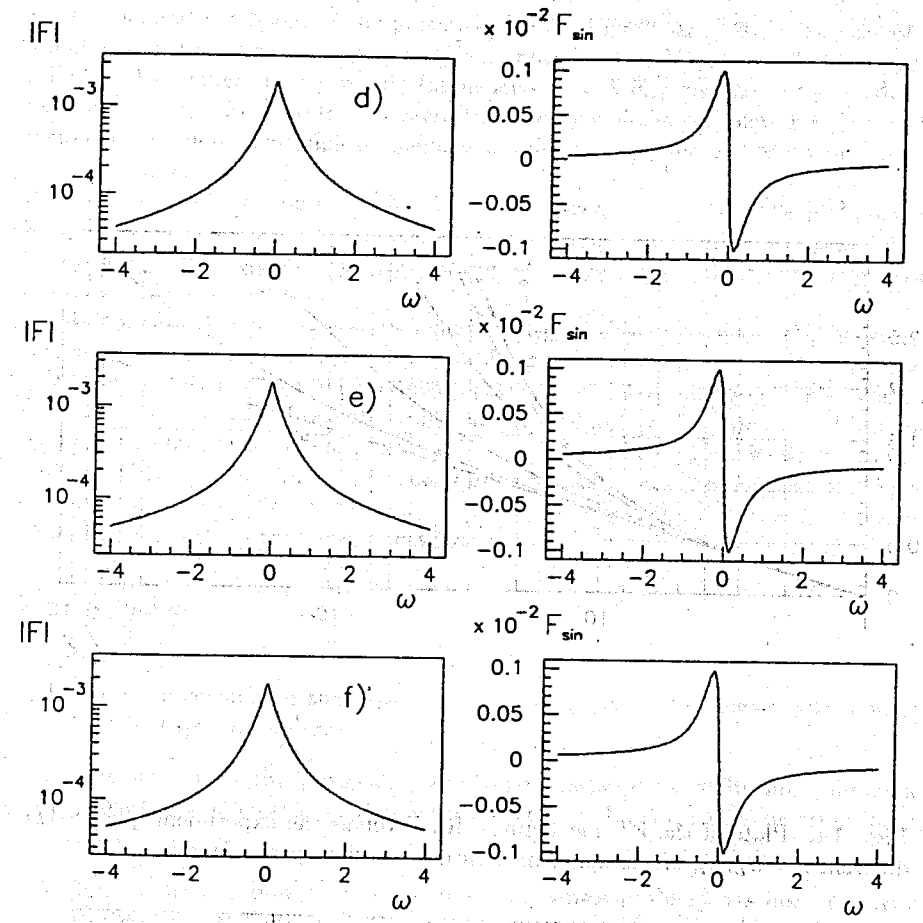

Fig. 13. The complete FT, $|F|$, and the partial FT, $F_{\sin}$, of the nonsymmetrical lorentzian spread functions, shown in Fig. 11, for last three parameters:

	d	e	f
σ_L	5.35	5.45	5.48
σ_R	0.15	0.05	0.02

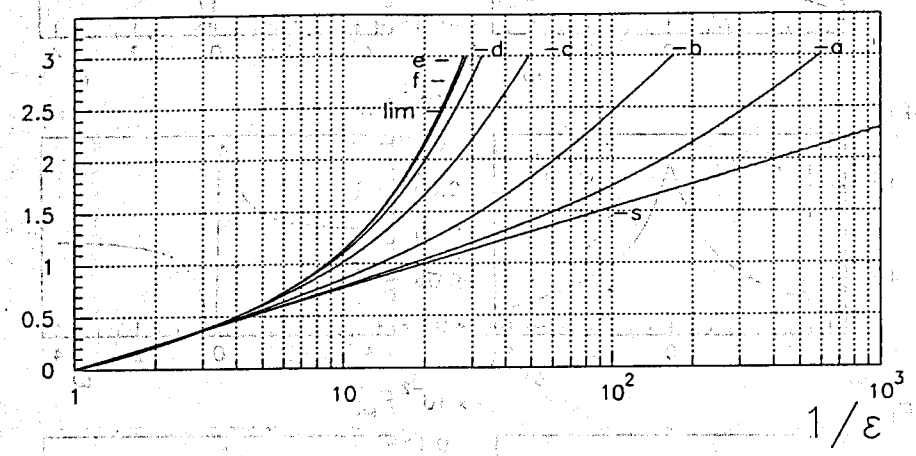

Fig. 14. Plots of the FT spectrum width Γ versus the experiment quality $1/\varepsilon$ for different $\kappa = \sigma_L/\sigma_R$ of the nonsymmetrical lorentzian spread function:

	a	b	c	d	e	f
$\kappa = \sigma_L/\sigma_R$	1.75	3.508	12.096	35.67	109.0	274.0

The general behaviour of the partial FT, $F_{\sin}$, (Figs 12 and 13) in the case of the lorentzians is the same as in the case of the gaussian (see Figs 6 and 7). The partial FT, $F_{\sin}$, has wings in the middle frequencies ω and $F_{\sin}$ maximum increases with ratio $\kappa = \sigma_L/\sigma_R$. Both factors increase the intensity of the complete FT, $|F|$, in the region of the middle and high frequencies ω, and thus increase the resolving power of the physical device.

The results of the computer simulation are given in Fig. 14. The FT spectrum width Γ is plotted versus the experiment quality $1/\varepsilon$ for symmetrical lorentzian (s), for six nonsymmetrical lorentzians (a, b, c, d, e, f) and for completely nonsymmetrical lorentzian (lim) with $\kappa = \infty$.

We see that at low values of the experiment quality $1/\varepsilon$ the difference between all these 8 curves is practically absent. The difference between physical devices is getting pronounced only for the experiment quality $1/\varepsilon \geq 3.5$. All possible FT spectrum widths Γ are restricted from above by the curve "lim", which corresponds to completely nonsymmetrical lorentzian with $\kappa = \infty$. The factor of merits of the physical device with nonsymmetrical lorentzian spread function over the physical device with symmetrical spread function is equal to 1.68:1 for $\varepsilon = 1/20$ and $\kappa = 12.096$ and is equal to 1.6:1 for $\varepsilon = 10^{-2}$ and $\kappa = 3.508$.

5. Conclusion

1. We have considered the resolving power of the physical device with nonsymmetrical spread function.
2. The quality of the physical device versus parameters of its nonsymmetrical spread function have been analyzed in term of the Fourier Transformation approach.
3. The computer simulation of the resolving power problem has been performed for two typical classes of the spread functions: gaussian and lorentzian.
4. It is shown that physical device with nonsymmetrical spread function demonstrates higher resolving power than the physical device with symmetrical spread function at the same total halfwidth.
5. It is shown that factor of merits of the physical device with nonsymmetrical spread function is the monotonic increasing function of $\kappa = \sigma_L/\sigma)R$, where σ_L and σ_R are the left and the right halfwidths of the left and of right parts of the given spread function, with limiting value at $\kappa = \infty$.
6. From two plots, one for gaussian and another for lorentzian, we may conclude that factor of merits of the physical device with nonsymmetrical gaussian is

higher than that of the physical device with nonsymmetrical lorentzian at the same experiment quality $1/\varepsilon$ and at ratio $\kappa = \sigma_L/\sigma_R$.

References

1. A. Papoulis, Systems and Transforms with Applications in Optics, Mc Graw-Hill Book Company, New York, 1968,
   см. русский перевод:
   А. Папулис, Теория систем и преобразований в оптике. "Мир", Москва, 1971.

2. R.J. Bell, Introductory Fourier Transform Spectroscopy, Academic Press, New York, 1972,
   см. русский перевод:
   Р.Дж. Белл, Введение в фурье-спектроскопию. "Мир", Москва, 1975.

3. L.M. Soroko, Fourier Transform Processing Algorithm of the Spectral Information in the Nuclear Physics, Communication JINR, 1–5030, 1970, Dubna.

Received by Publishing Department
on July 10, 1997.